

Oxygen-dependent hyperpolarized ^{129}Xe brain MR

Haidong Li[†], Zhiying Zhang[†], Jianping Zhong, Weiwei Ruan, Yeqing Han, Xianping Sun, Chaohui Ye and Xin Zhou*



Hyperpolarized (HP) ^{129}Xe MR offers unique advantages for brain functional imaging (fMRI) because of its extremely high sensitivity to different chemical environments and the total absence of background noise in biological tissues. However, its advancement and applications are currently plagued by issues of signal strength. Generally, xenon atoms found in the brain after inhalation are transferred from the lung via the bloodstream. The longitudinal relaxation time (T_1) of HP ^{129}Xe is inversely proportional to the pulmonary oxygen concentration in the lung because oxygen molecules are paramagnetic. However, the T_1 of ^{129}Xe is proportional to the pulmonary oxygen concentration in the blood, because the higher pulmonary oxygen concentration will result in a higher concentration of diamagnetic oxyhemoglobin. Accordingly, there should be an optimal pulmonary oxygen concentration for a given quantity of HP ^{129}Xe in the brain. In this study, the relationship between pulmonary oxygen concentration and HP ^{129}Xe signal in the brain was analyzed using a theoretical model and measured through *in vivo* experiments. The results from the theoretical model and experiments in rats are found to be in good agreement with each other. The optimal pulmonary oxygen concentration predicted by the theoretical model was 21%, and the *in vivo* experiments confirmed the presence of such an optimal ratio by reporting measurements between 25% and 35%. These findings are helpful for improving the ^{129}Xe signal in the brain and make the most of the limited spin polarization available for brain experiments. Copyright © 2016 John Wiley & Sons, Ltd.

Additional supporting information may be found in the online version of this article at the publisher's web site.

Keywords: hyperpolarized ^{129}Xe ; brain MRI; oxygen concentration; SEOP

INTRODUCTION

The technique of spin-exchange optical pumping (SEOP) with noble gases (^{129}Xe , ^3He and ^{83}Kr) can result in signal enhancements of four to five orders of magnitude compared with signals in the thermal equilibrium (1–3). The non-equilibrium nuclear spin polarization (hyperpolarization) and the biological inertness of the noble gases result in unique advantages for MR in biological systems. Hyperpolarized noble gas pulmonary MRI and NMR have achieved rapid development since its first demonstration in excised mouse lung (4–9). The isotopes ^{129}Xe and ^3He ($I = 1/2$) are the most commonly used for pulmonary MRI because they have a relatively long longitudinal relaxation time and a higher polarization compared with quadrupole nuclei ^{83}Kr . Hyperpolarized ^{129}Xe MRI has great potential for the study of brain function due to: (i) the absence of a background MR signal for xenon in the biological tissues; (ii) the high sensitivity of the ^{129}Xe chemical shift to different chemical environments in various tissues; and (iii) the high lipid solubility of xenon in biological tissue and Ostwald solubility in red blood cells and plasma (0.2 and 0.1, respectively) (10). As a result of these benefits, hyperpolarized ^{129}Xe has been successfully used for brain MRI by research groups (11–13). Recently, Zhou and co-workers successfully detected the stroke area in a rat brain using hyperpolarized ^{129}Xe (14); Mazzanti and co-workers applied hyperpolarized xenon for brain functional imaging (fMRI) and demonstrated the feasibility of detecting brain function changes using hyperpolarized ^{129}Xe (15). However, the applications of hyperpolarized ^{129}Xe to brain MRI has not progressed as rapidly

as its applications to the lung. The main challenge towards the advancement is the low signal of hyperpolarized ^{129}Xe in the brain, which is limited by the low solubility of xenon in the brain tissue. Generally, there are two ways to deliver xenon to the brain. The first is the direct injection of hyperpolarized xenon dissolved in lipid emulsions into the internal carotid artery, which is an invasive method (16). Moreover, the amount of hyperpolarized xenon available is limited by the allowed volume of injectable solution and the solution-tissue partition coefficient. The second method, which is non-invasive and widely used, involves inhaling hyperpolarized ^{129}Xe gas through the lung (11–13,17). The inhaled hyperpolarized xenon first enters the lung while in the gas phase, and then diffuses across the alveolar walls and enters the pulmonary capillaries. Afterwards, hyperpolarized

* Correspondence to: Professor Xin Zhou, National Center for Magnetic Resonance in Wuhan, Wuhan Institute of Physics and Mathematics, Chinese Academy of Sciences, 30 West Xiaohongshan, Wuhan, China.
E-mail: xinzhou@wipm.ac.cn

H. Li, Z. Zhang, J. Zhong, W. Ruan, Y. Han, X. Sun, C. Ye, X. Zhou
Key Laboratory of Magnetic Resonance in Biological Systems, State Key Laboratory of Magnetic Resonance and Atomic and Molecular Physics, National Center for Magnetic Resonance in Wuhan, Wuhan Institute of Physics and Mathematics, Chinese Academy of Sciences, Wuhan, 430071, China

[†] These authors contributed equally to this work.

Abbreviations used: fMRI, functional MRI; HP, hyperpolarized; SEOP, spin-exchange optical pumping; SNR, signal-to-noise ratio; $p_{\text{A}}\text{O}_2$, alveolar oxygen partial pressure.

xenon in the dissolved phase is transported into the brain via the bloodstream. As the xenon concentration in brain tissue reaches saturation, the ^{129}Xe signal from the brain mainly depends on the initial ^{129}Xe polarization in the gas phase and any relaxation occurring during the delivery of ^{129}Xe to the brain tissue. Although recent improvements in SEOP techniques have led to higher polarization levels and signals (2,18), the required modifications to most typical ^{129}Xe polarizers are not straightforward. Alternatively, an efficient and convenient approach is to minimize relaxation of ^{129}Xe during the entire delivery process. By way of a large number of experiments in hyperpolarized ^{129}Xe brain MRI, we found that the gas mixtures containing different oxygen concentrations to ventilate rats lead to significant changes in brain ^{129}Xe signal. This is mainly because: (i) a higher oxygen-level ventilation results in faster relaxation of hyperpolarized ^{129}Xe gas in the lung (19), (ii) while the higher pulmonary oxygenation partial pressure lengthens the longitudinal relaxation time of dissolved ^{129}Xe in the blood by increasing the concentration of diamagnetic oxyhemoglobin and decreasing the concentration of paramagnetic deoxyhemoglobin (20–23). The flow chart (as shown in Supplementary Material Fig. 1) for delivering hyperpolarized xenon from the lung to the brain, showing different components contributing to the relaxation of hyperpolarized ^{129}Xe .

In this study, HP ^{129}Xe signals in the brain were investigated as a function of various pulmonary oxygen concentrations using numerical simulation and *in vivo* experiments in rats. The consistent pulmonary oxygen concentration dependence of the hyperpolarized ^{129}Xe MR signal in the brain was observed using both methods, and the optimal oxygen concentration was also obtained. These results offer a new way to improve the hyperpolarized ^{129}Xe MR signal in the brain by reducing the hyperpolarized ^{129}Xe longitudinal relaxation rate during transportation to the brain tissues, which is an important step to expedite the applications of hyperpolarized ^{129}Xe *in vivo* brain MRI studies in the future.

MATERIALS AND METHODS

The theoretical simulations

Based on the Kety–Schmidt theory (24), the model of hyperpolarized ^{129}Xe delivered to the brain tissue by ventilation has been derived by Peled and co-workers (25). They provide the

following equation to describe the hyperpolarized ^{129}Xe MR signal in the brain in the steady-state:

$$S_{\text{BrainTissue-Steady}} = \frac{C_i e^{-\frac{t_i}{T_{1\text{blood}}}} \lambda R_F F_i}{\left(R_F + \frac{V_A}{T_{1\text{alveoli}}} + \lambda Q\right) \left(\frac{F_i}{\lambda_i} + \frac{1}{T_{1i}}\right)} \quad [1]$$

where C_i is the inhaled concentration of hyperpolarized ^{129}Xe and t_i is the hyperpolarized ^{129}Xe transit time in the blood. $T_{1\text{blood}}$, $T_{1\text{alveoli}}$ and T_{1i} are hyperpolarized ^{129}Xe longitudinal relaxation times in the blood, alveoli and brain tissue, respectively. λ is the partition coefficient for xenon between blood and gas, R_F is the constant rate of gas exchange, F_i is the blood flow to the brain tissue, V_A is the alveolar volume, Q is the pulmonary blood flow, and λ_i is the partition coefficient for xenon between tissue and blood. The parameters used for the analytical mode are shown in Table 1. $T_{1\text{alveoli}}$ is inversely proportional to the pulmonary oxygen concentration. $T_{1\text{blood}}$ is proportional to the pulmonary oxygen concentration that ranged from 10% to 21%, corresponding to the alveolar oxygen partial pressure, $p_{\text{A}}\text{O}_2$, that ranged from 30 to 100 mmHg. $T_{1\text{blood}}$ in the deoxygenated blood and oxygenated blood of 4 s and 13 s are used for the linear scale (20,22), and $T_{1\text{blood}}$ is considered as a constant when oxygen is saturated in blood, i.e., the $p_{\text{A}}\text{O}_2$ is above 100 mmHg (22).

Animals preparation

All surgical and experimental procedures were approved by our institutional animal care and use committee. Healthy Sprague–Dawley rats weighing 180–240 g were anesthetized using 5% isoflurane using an induction chamber. The endotracheal intubation was accomplished with a 14-gauge, 3-cm catheter, followed by adjustment of the isoflurane concentration to 1.5% to maintain a sufficient depth of anesthesia. The rats were ventilated with

Table 1. Parameters used in the analytical model

	R_F (ml/min)	V_A (ml)	Q (ml/s)	λ	λ_i	F_i (ml/100 g/min)
Values	187	3	1.5	0.17	1.015	106
Ref. #	(28)	(29)	(30)	(31)	(32)	(32)

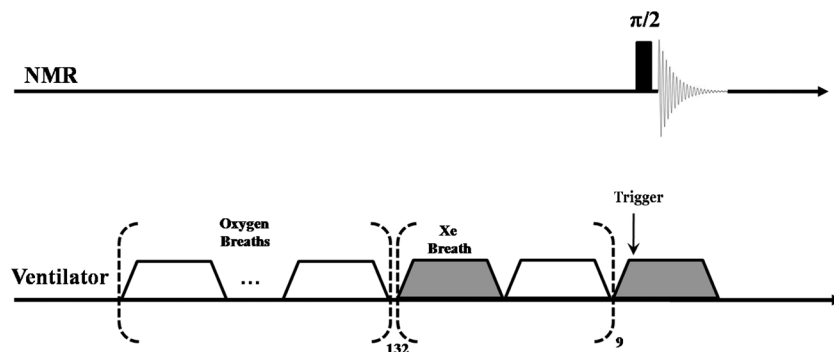


Figure 1. Schematic diagram of the ventilation strategy. Hyperpolarized xenon and oxygen were ventilated to rats alternately 10 times and data was acquired during the 10th xenon breathholding. Before inhaling xenon, 132 times of oxygen mixture respiration were needed to remove the remaining xenon from the body.

various oxygen concentrations (oxygen-nitrogen mixtures). Ventilation with HP xenon was accomplished using a homebuilt MR-compatible delivery system. In order to keep the rats' physiological conditions constant during the experiments, the respiratory rate was set to 43 breaths per minute for both oxygen and xenon (350 ms for inhalation, 200 ms for breath-holding and 850 ms for exhalation). During the experiments, the rats' oxygen saturation and heart rate were monitored using a pulse oximeter (MouseOx[®]Plus Systems; Harvard Apparatus, Holliston, MA, USA) via a pair of optical transducers placed on the hind paw. Body temperature was regulated using a heat therapy pump via water circulating pads. After the experiments, the rats were sacrificed with an intraperitoneal injection of pentobarbital sodium (200 mg/kg).

Hyperpolarized xenon gas preparation and delivery

Hyperpolarized xenon was produced by the technique of SEOP using a homebuilt polarizer system (26,27). The polarizer system equipped with a 75 W narrowed-width laser diode array (QPC Lasers Inc., CA, USA) worked in the flow-through mode. A gas mixture consisting of 1% natural abundance xenon (26% ¹²⁹Xe), 10% N₂ and 89% ⁴He was used. The gas mixture flowed through the glass optical cell in the opposite direction of the laser beam at a flow rate of 0.4 standard liters per minute at a pressure of ~70 PSIG. After polarization, the available nuclear spin polarization of xenon was measured to be ~20%. The gas mixture was then flowed through a cold glass trap, which was immersed in liquid nitrogen and surrounded with a 200-mT magnetic field provided by a permanent magnet. Hyperpolarized xenon was stored in the solid state in the trap because of its higher frozen point while other gases (nitrogen and helium) flowed out of the mixture. After this accumulation process, hyperpolarized xenon was thawed using hot water and expanded into a 350-ml Tedlar bag, which was purged to 10 Pa by a vacuum pump prior to the cycle. The available spin polarization of xenon in the Tedlar bag was approximately 10%.

The Tedlar bag containing hyperpolarized xenon was placed in a pressure chamber and connected to a homebuilt MR-compatible delivery system. Controlled by a data acquisition card and LabVIEW script (National Instruments Corporation, Austin, TX, USA), the delivery system was ready to ventilate rats HP xenon gas or oxygen mixture gas as needed. The ventilation was controlled using a switch, which also controlled the durations of the pneumatic control valves' states. The latter was driven by high purity nitrogen gas. The delivery system can also trigger the MRI scanner to start the acquisition during breathhold after inhalation of hyperpolarized xenon by the rats.

The apparent relaxation time (T_{0-c})

Before connection to the delivery system, hyperpolarized ¹²⁹Xe is depolarized after being thawing from ice to gas and transferred to the Tedlar bag manually. The depolarization is difficult to quantify. Thus, the impact of different pulmonary oxygen concentrations on the ¹²⁹Xe signal in the brain based on measurements of the intensity of dissolved xenon signal is difficult. To overcome this problem, we instead propose the use of a relaxation time, "T_{0-c}", to evaluate the influence of different pulmonary oxygen concentrations on hyperpolarized ¹²⁹Xe signal in brain tissue. The relaxation time "T_{0-c}" is an apparent longitudinal relaxation time, covering all relaxation process incurred during hyperpolarized xenon transport from the container to the brain. T_{0-c} includes

the relaxation in the Tedlar bag where xenon is kept after being thawed from ice to gas. It also includes relaxation in the lung where ¹²⁹Xe enters the pulmonary capillary, the relaxation in the blood where the ¹²⁹Xe was transferred from the lung to the brain and the relaxation of ¹²⁹Xe in the brain tissue where the hyperpolarized ¹²⁹Xe signal was measured. The apparent relaxation time (T_{0-c}) is not sensitive to the initial polarization and is instead affected only by the environment of xenon during transportation from the lung to the brain. This apparent relaxation time (T_{0-c}) was used to evaluate the influence of the pulmonary oxygen concentration on the hyperpolarized ¹²⁹Xe brain signal in *in-vivo* experiments, and the relationship between the HP ¹²⁹Xe signal of the brain and the relaxation time can be written as:

$$S_{BrainTissue} = S_0 \cdot \exp(-t_0/T_{0-c}) \quad [2]$$

where S₀ is the initial hyperpolarized ¹²⁹Xe signal in the brain and t₀ is the time that xenon spends in transit to the brain tissue after exiting from the Tedlar bag.

MR data acquisition

All MR spectra were carried out on a Bruker Biospec 4.7 T MRI system using a horizontal, 30-cm bore magnet (Oxford Instruments, Oxford, UK) equipped with a 200 mT/m shielded gradient (B-GA12S). The data were collected using a homebuilt dual-tuned surface coil, which was tuned to the ¹H and ¹²⁹Xe resonances (200.29 and 55.4 MHz, respectively). Before data acquisition, the rat was ventilated with hyperpolarized xenon and oxygen-nitrogen mixtures alternately to achieve a steady ¹²⁹Xe MR signal in the brain (13). During the breath-hold step of the 10th hyperpolarized xenon ventilation, the MRI scanner was triggered by the delivery system to start collecting data (shown in Fig. 1). The excitation RF pulse was centered at the dissolved ¹²⁹Xe signal (195 ppm downfield from the gas phase) with a flip angle of 90 degrees. The bandwidth of acquisition was 25 KHz, and the number of sampled points was 1024. After acquisition, the rat was ventilated with an oxygen-nitrogen mixture 132 times (~3 min, i.e., five times the time that xenon totally decays after the stop of xenon ventilation) to remove the residual dissolved xenon from the body in order to prepare the rats in the same initial physical condition (13). For each rat, nine spectra were acquired within the same interval in the same way for fitting the xenon's apparent longitudinal relaxation time. Six different oxygen concentration mixtures (i.e., 21% O₂ + 79% N₂, 35% O₂ + 65% N₂, 50% O₂ + 50% N₂, 70% O₂ + 30% N₂, 80% O₂ + 20% N₂ and 100% O₂) were used in this study to obtain the optimal pulmonary oxygen concentration. To reduce rat-to-rat variability, four sets of data were collected from four separate rats for each value of the oxygen concentration.

Data processing

The spectra were processed using the Topspin 2.0 software (Bruker Biospin Co., Billerica, MA, USA). Before Fourier transform, a 20-Hz exponential line-broadening filter was applied to each free induction decay to reduce the noise and improve the signal-to-noise ratio (SNR). Then the integral of the area under the dissolved ¹²⁹Xe peaks, which was regarded as the signal intensity of dissolved ¹²⁹Xe, was calculated after phase correction. The signal intensity was normalized and fitted to the fitting function in MATLAB (MathWorks, Natick, MA, USA) to obtain the apparent relaxation time (T_{0-c}) for each oxygen concentration. Each data

point for fitting the T_{O-c} decay curve was normalized by the first data acquired points in the experiment before averaging. To make the curve reflect the real relaxation time as a function of oxygen concentration and to reduce the rat-to-rat variability, each data point for fitting was averaged across four independent rats. Six different oxygen concentrations (100%, 85%, 70%, 50%, 35% and 21%) were used for ventilating rats in these experiments. The data were fitted to the function $y = A \cdot \exp(-t/T_{O-c})$ to obtain the apparent relaxation time (T_{O-c}).

RESULTS

Theoretical simulations

First, an analytical model depicting ^{129}Xe polarization traveling from the ventilator to the rat brain was developed. The model predicted the optimal pulmonary oxygen concentration for the brain ^{129}Xe MR signal to be 21%. The brain ^{129}Xe signal rose with the increase of pulmonary oxygen concentration when the concentration was less than 21%, and decreased with further increases in oxygen concentration in the lung (see Fig. 2). Moreover, the brain ^{129}Xe signal varied with pulmonary oxygen concentration non-linearly before the concentration reached the optimal one, and decreased linearly with further increases of oxygen concentrations.

Oxygen concentration in the lung

In this study, gas mixtures containing various oxygen concentrations and HP xenon were ventilated to rats alternately, similar to the ventilation mode demonstrated in previous studies (14,15). Before data collection, the rat was ventilated with HP xenon and oxygen–nitrogen mixtures alternately nine times to achieve a steady ^{129}Xe signal in the brain. Because the rat was ventilated with a xenon and oxygen mixture alternately, and there are always residual gases in the pulmonary alveoli, the pulmonary oxygen concentration was not equal to the ventilated concentration. In this study, both the tidal volume of xenon and the oxygen–nitrogen mixture are about the same as the residual

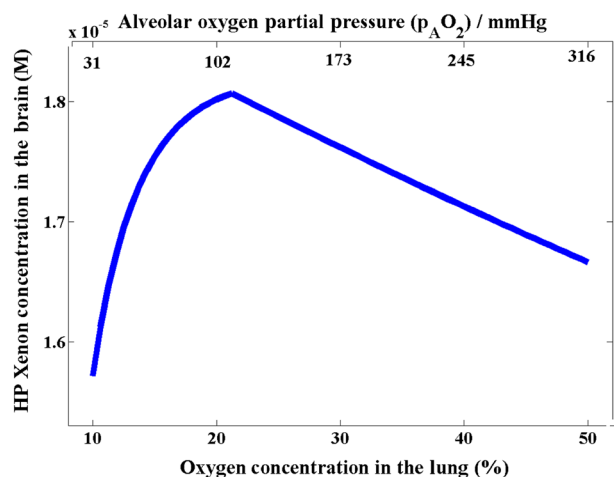


Figure 2. Dependence of hyperpolarized (HP) xenon concentration in the brain on the pulmonary oxygen concentration predicted by the theoretical model. The concentration of HP xenon in the brain first increases non-linearly and then decreases linearly with increasing pulmonary oxygen concentration. The optimal pulmonary oxygen concentration for the HP xenon brain MR signal was 21%.

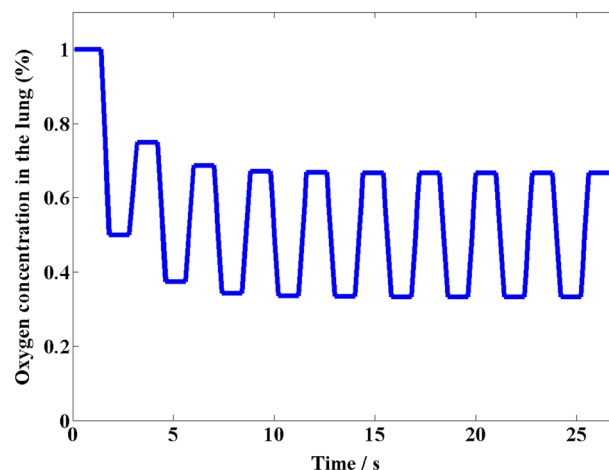


Figure 3. Variation of the oxygen concentration in the lung with the time at which the rat breathes hyperpolarized (HP) xenon and oxygen–nitrogen gas mixtures alternately. The mean pulmonary oxygen concentration was steady after breathing HP xenon and oxygen mixture gas twice. The value was half of the concentration of the ventilated gas mixture. The oxygen concentration of the ventilated gas mixture shown in this figure was 100%, i.e., pure oxygen.

gas volume in the lung, i.e., 3 ml. The pulmonary oxygen concentration reaches a stable state relative to the oxygen concentration of respiratory gas during the process of ventilation. Fig. 3 shows the simulation of pulmonary oxygen concentration over time after the rats were ventilated with hyperpolarized xenon and oxygen–nitrogen mixtures. The mean pulmonary oxygen concentration was steady after the rat inhaled xenon and oxygen mixtures twice. The concentration value was half of the concentration of the ventilated gas mixture.

Measurement of T_{O-c}

Fig. 4 shows the typical dynamics of HP ^{129}Xe spectra in the brain. As time increases, the HP ^{129}Xe signal in the brain decreases, as

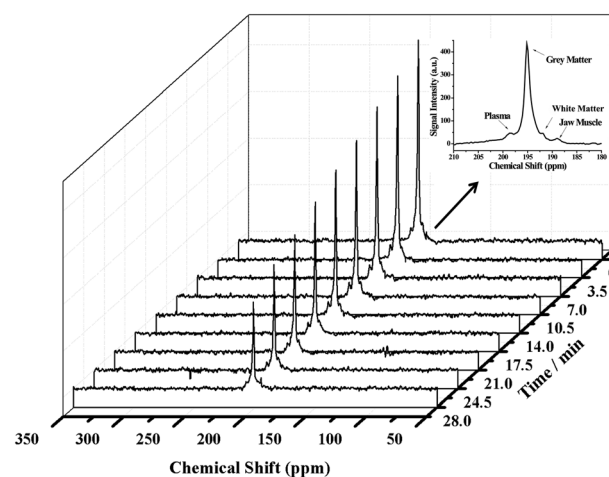


Figure 4. The typical dynamic spectra of the hyperpolarized (HP) xenon MR signal in the brain, which was measured in the rat. HP xenon signal decreased with the increasing interval time. The inset showed the assignments of the visible dissolved ^{129}Xe peaks in the brain, and the signals at 189 ppm and 195 ppm are from the jaw muscle and grey matter (33), respectively. The other two signals at 192 ppm and 197 ppm are mostly likely from the white matter (33) and plasma (20), respectively.

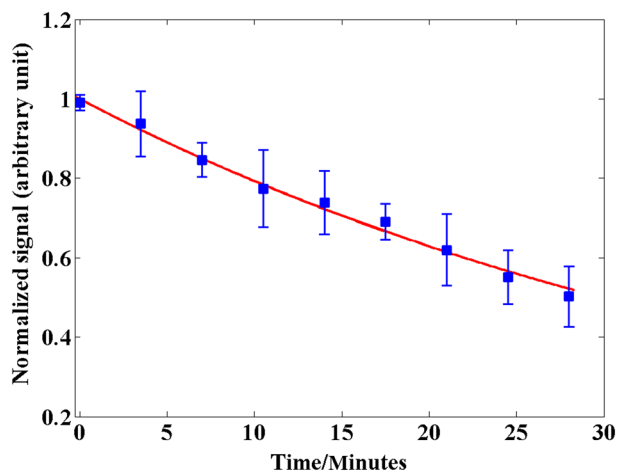


Figure 5. The typical result of “ T_{O-C} ” data fitting under the oxygen concentration 85%, which showed a good exponential fitting degree in the data acquired from *in vivo* experiments.

expected. Fig. 5 shows the typical “ T_{O-C} ” fitting curve under the ventilated oxygen concentration of 85%. The apparent relaxation times T_{O-C} measured for different pulmonary oxygen concentration, i.e. 50%, 42.5%, 35%, 25%, 17.5%, 10.5%, were 36.5 ± 2.8 min, 43.0 ± 2.2 min, 45.9 ± 4.4 min, 46.0 ± 4.3 min, 41.7 ± 2.6 min and 35.5 ± 3.9 min, respectively.

Variation of T_{O-C} with pulmonary oxygen concentration

The measured apparent relaxation time (T_{O-C}) from *in vivo* experiments increased with the increasing pulmonary oxygen concentration before the oxygen concentration in the lung reached 25%. However, when the oxygen concentration exceeded 25%, T_{O-C} decreased with concentration (shown in Fig. 6). The optimal pulmonary oxygen concentration for the hyperpolarized ^{129}Xe signal in brain was found to range from 25% to 35% (i.e., corresponding to the oxygen concentration in the gas mixture for breathing of 50-70% under the current ventilation mode) obtained in this study, which is a little higher than that obtained from the numerical simulation.

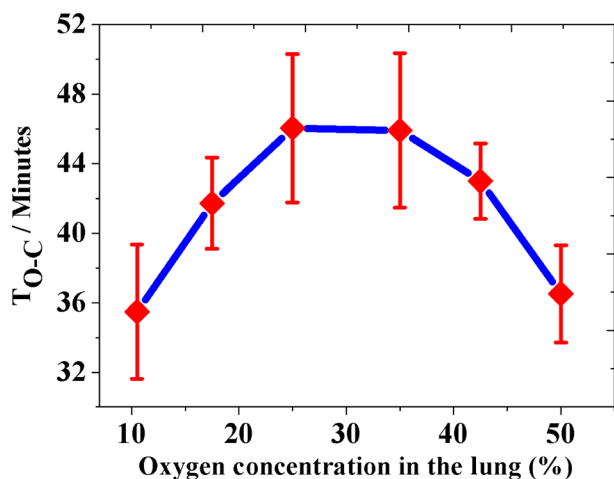


Figure 6. Relationship between the measured T_{O-C} from *in vivo* experiments and pulmonary oxygen concentration. The value of T_{O-C} first increases and then decreases with the pulmonary oxygen concentration.

DISCUSSION

In this study, a more reliable and accurate parameter, the apparent relaxation time (T_{O-C}), is proposed to quantify the influence of various pulmonary oxygen concentrations on hyperpolarized ^{129}Xe signal in the brain. The ^{129}Xe signal intensity in the brain is affected by the initial polarization of xenon in the *in vivo* experiments. Consequently, the initial polarization of xenon gas in the Tedlar bag was hard to quantify accurately as a result of the fluctuation of the xenon polarizer and the manual process of xenon ice thawing into gas. The apparent relaxation time (T_{O-C}), which takes into account all the relaxation during xenon delivered from the Tedlar bag to the brain, is not sensitive to the initial polarization. Moreover, in all our experiments, the same delivery system and ventilation strategy were utilized. The same Tedlar bag was purged with a vacuum system to the same pressure (10 Pa). The only conditions that were allowed to vary were the oxygen concentration of the gas mixture for ventilation and the naturally variable rat physiology. To avoid differences from rat to rat, four rats were used when measuring each oxygen concentration. The apparent relaxation time (T_{O-C}) was found to be dominated by the oxygen concentration. Therefore, the apparent relaxation time (T_{O-C}) can be utilized to explain the influence of the pulmonary oxygen concentration on the brain ^{129}Xe signal, more reliably and accurately. T_{O-C} is a useful parameter to optimize the amount of oxygen inhaled along with xenon in cases where the partial pressure of oxygen in the lungs is below 100 mmHg. However, when the oxygen is added in the xenon gas, the time that hyperpolarized ^{129}Xe spent in the Tedlar bag would have to be kept very short.

The optimal pulmonary oxygen concentration obtained from the theoretical model was in good agreement with the oxygen concentration of the air used. The simulated ^{129}Xe signal was based on the known ^{129}Xe relaxation time in the blood ($T_{1\text{blood}}$) and alveoli ($T_{1\text{alveoli}}$). $T_{1\text{alveoli}}$ was inversely proportional to the oxygen concentration, and the higher oxygen concentration in the lung, the shorter $T_{1\text{alveoli}}$ (19). The ^{129}Xe relaxation time in blood, $T_{1\text{blood}}$, was proportional to the oxygen concentration only when the blood was not saturated by oxygen, i.e., when the oxygen partial pressure in the blood was lower than 100 mmHg. When the oxygen concentration in the lung exceeded 21%, the $T_{1\text{blood}}$ was considered constant in this study. The ^{129}Xe signal was then proportional to $T_{1\text{alveoli}}$, and with the concentration increasing, the signal intensity decreased, which makes the ^{129}Xe signal vary with oxygen concentration linearly when the concentration exceeded 21%. This makes sense because, under normal conditions, the blood oxygen saturation was approximately 100% in rats and humans by breathing air.

The optimal pulmonary oxygen concentration obtained from the experiment was a little higher than that achieved from the theoretical model. In the theoretical model, the consumption of oxygen by organs, blood and other physiological activities were not considered. Also, the concentration was constant during xenon transporting within the body. During *in vivo* experiments, oxygen is consumed to maintain normal physiological activities. Consequently, the blood is not totally saturated when the oxygen concentration in the lung was 21%. Indeed, a higher concentration is needed to saturate the blood.

The ventilation strategy used in this study, i.e., ventilating rats with oxygen mixtures and hyperpolarized xenon alternately, was similar to strategies reported in previous studies. In this ventilation strategy, the mean oxygen concentration in the lung was approximately half that in the gas mixture used for the rats ventilation.

Moreover, oxygen and HP xenon concentrations in the lung varied with ventilation time, which may cause fluctuations of HP ^{129}Xe signals in the brain. To avoid possible fluctuations caused by the ventilation, the data acquisition in this study was done at the same time point during the ventilation, i.e., at the beginning of the breath hold of the 10th cycle of xenon inhalation.

CONCLUSION

The influence of the pulmonary oxygen concentration on the hyperpolarized ^{129}Xe signal in the brain was studied by both numerical simulation and *in vivo* experiments. A more reliable and accurate parameter, the apparent relaxation time (T_{0-c}), is proposed to evaluate the dependence of the hyperpolarized ^{129}Xe signal in the brain on the pulmonary oxygen concentration. The results obtained from the two methods were consistent with each other. The optimal pulmonary oxygen concentration predicted with the theoretical model was confirmed by *in vivo* rat experiments. The optimal pulmonary oxygen concentration for *in vivo* hyperpolarized ^{129}Xe brain imaging ranged from 25% to 35%. These results should help in the design of experiments that maximize the utility of the limited available ^{129}Xe nuclear spin polarization. This would help expedite the application of hyperpolarized ^{129}Xe to brain fMRI.

Acknowledgements

This work was supported by the Natural Science Foundation of China (81227902).

REFERENCES

- Walker TG, Happer W. Spin-exchange optical pumping of noble-gas nuclei. *Rev. Mod. Phys.* 1997; 69: 629–42.
- Nikolaou P, Coffey AM, Walkup LL, Gust BM, Whiting N, Newton H, Barcus S, Muradyan I, Dabaghyan M, Moroz GD, Rosen MS, Patz S, Barlow MJ, Chekmenev EY, Goodson BM. Near-unity nuclear polarization with an open-source ^{129}Xe hyperpolarizer for NMR and MRI. *Proc. Natl. Acad. Sci. U. S. A.* 2013; 110: 14150–5.
- Pavlovskaya GE, Cleveland ZI, Stupic KF, Basaraba RJ, Meersmann T. Hyperpolarized krypton-83 as a contrast agent for magnetic resonance imaging. *Proc. Natl. Acad. Sci. U. S. A.* 2005; 102: 18275–9.
- Albert MS, Cates GD, Driehuys B, Happer W, Saam B, Springer CS, Wishnia A. Biological magnetic resonance imaging using laser-polarized Xe-129. *Nature* 1994; 370: 199–201.
- Driehuys B, Cofer GP, Pollaro J, Mackel JB, Hedlund LW, Johnson GA. Imaging alveolar-capillary gas transfer using hyperpolarized Xe-129 MRI. *Proc. Natl. Acad. Sci. U. S. A.* 2006; 103: 18278–83.
- Mugler JP, Altes TA, Ruset IC, Dregely IM, Mata JF, Miller GW, Ketel S, Ketel J, Hersman FW, Ruppert K. Simultaneous magnetic resonance imaging of ventilation distribution and gas uptake in the human lung using hyperpolarized xenon-129. *Proc. Natl. Acad. Sci. U. S. A.* 2010; 107: 21707–12.
- Stewart NJ, Leung G, Norquay G, Marshall H, Parra-Robles J, Murphy PS, Schulte RF, Elliot C, Condliffe R, Griffiths PD, Kiely DG, Whyte MK, Wolber J, Wild JM. Experimental validation of the hyperpolarized ^{129}Xe chemical shift saturation recovery technique in healthy volunteers and subjects with interstitial lung disease. *Magn. Reson. Med.* 2014; 74: 196–207.
- Qing K, Mugler JP, Altes TA, Jiang Y, Mata JF, Miller GW, Ruset IC, Hersman FW, Ruppert K. Assessment of lung function in asthma and COPD using hyperpolarized ^{129}Xe chemical shift saturation recovery spectroscopy and dissolved-phase MRI. *NMR Biomed.* 2014; 27: 1490–501.
- Fox MS, Ouriadov A, Thind K, Hegarty E, Wong E, Hope A, Santyr GE. Detection of radiation induced lung injury in rats using dynamic hyperpolarized Xe-129 magnetic resonance spectroscopy. *Med. Phys.* 2014; 41: 072302.

- Ladefoge J, Andersen AM. Solubility of xenon-133 at 37 °C in water, saline, olive oil, liquid paraffin, solutions of albumin, and blood. *Phys. Med. Biol.* 1967; 12: 353–8.
- Kilian W, Seifert F, Rinneberg H. Dynamic NMR spectroscopy of hyperpolarized ^{129}Xe in human brain analyzed by an uptake model. *Magn. Reson. Med.* 2004; 51: 843–7.
- Imai H, Kimura A, Akiyama K, Ota C, Okimoto K, Fujiwara H. Development of a fast method for quantitative measurement of hyperpolarized ^{129}Xe dynamics in mouse brain. *NMR Biomed.* 2012; 25: 210–7.
- Zhou X, Mazzanti M, Chen J, Tzeng YS, Mansour J, Gereige J, Venkatesh A, Sun Y, Mulkern R, Albert M. Reinvestigating hyperpolarized ^{129}Xe longitudinal relaxation time in the rat brain with noise considerations. *NMR Biomed.* 2008; 21: 217–25.
- Zhou X, Sun Y, Mazzanti M, Henninger N, Mansour J, Fisher M, Albert M. MRI of stroke using hyperpolarized ^{129}Xe . *NMR Biomed.* 2011; 24: 170–5.
- Mazzanti ML, Walvick RP, Zhou X, Sun Y, Shah N, Mansour J, Gereige J, Albert MS. Distribution of hyperpolarized xenon in the brain following sensory stimulation: preliminary MRI findings. *PLoS One* 2011; 6: e21607.
- Duhamel G, Choquet P, Grillon E, Lamalle L, Leviel JL, Ziegler A, Constantinesco A. Xenon-129 MR imaging and spectroscopy of rat brain using arterial delivery of hyperpolarized xenon in a lipid emulsion. *Magn. Reson. Med.* 2001; 46: 208–12.
- Swanson SD, Rosen MS, Agranoff BW, Coulter KP, Welsh RC, Chupp TE. Brain MRI with laser-polarized ^{129}Xe . *Magn. Reson. Med.* 1997; 38: 695–8.
- Ruset IC, Ketel S, Hersman FW. Optical pumping system design for large production of hyperpolarized Xe-129. *Phys. Rev. Lett.* 2006; 96: 053002.
- Möller HE, Chen XJ, Saam B, Hagspiel KD, Johnson GA, Altes TA, de Lange EE, Kauczor HU. MRI of the lungs using hyperpolarized noble gases. *Magn. Reson. Med.* 2002; 47: 1029–51.
- Albert MS, Balamore D, Kacher DF, Venkatesh AK, Jolesz FA. Hyperpolarized ^{129}Xe T_1 in oxygenated and deoxygenated blood. *NMR Biomed.* 2000; 13: 407–14.
- Wolber J, Cherubini A, Leach MO, Bifone A. On the oxygenation-dependent ^{129}Xe T_1 in blood. *NMR Biomed.* 2000; 13: 234–7.
- Norquay G, Leung G, Stewart NJ, Tozer GM, Wolber J, Wild JM. Relaxation and exchange dynamics of hyperpolarized ^{129}Xe in human blood. *Magn. Reson. Med.* 2014; 74: 303–11.
- Wolber J, Cherubini A, Leach MO, Bifone A. Hyperpolarized ^{129}Xe NMR as a probe for blood oxygenation. *Magn. Reson. Med.* 2000; 43: 491–6.
- Kety SS. The theory and applications of the exchange of inert gas at the lungs and tissues. *Pharmacol. Rev.* 1951; 3: 1–41.
- Peled S, Jolesz FA, Tseng CH, Nascimben L, Albert MS, Walsworth RL. Determinants of tissue delivery for ^{129}Xe magnetic resonance in humans. *Magn. Reson. Med.* 1996; 36: 340–4.
- Zhou X. Hyperpolarized noble gases as contrast agents. In *In vivo NMR Imaging*, Schröder L, Faber C (eds). Humana Press: New Jersey, 2011, pp. 189–204.
- Zhou X, Sun X, Luo J, Zeng X, Liu M, Zhan M. Production of hyperpolarized ^{129}Xe gas without nitrogen by optical pumping at ^{133}Cs D_2 line in flow system. *Chin. Phys. Lett.* 2004; 21: 1501.
- Krinke GJ. *The Laboratory Rat*. Bullock GR, Bunton T (eds). San Diego, CA: Academic Press, 2000.
- Lai YL, Hildebrandt J. Respiratory mechanics in the anesthetized rat. *J. Appl. Physiol.* 1978; 45: 255–60.
- Austgen TR, Plumley DA, Souba WW. Simple method of determining pulmonary blood flow in the anesthetized rat. *J. Invest. Surg.* 1991; 4: 81–6.
- Chen RY, Fan FC, Kim S, Jan KM, USAMI S, Chien S. Tissue-blood partition coefficient for xenon: temperature and hematocrit dependence. *J. Appl. Physiol.* 1980; 49: 178–83.
- Gjedde A, Caronna JJ, Hindfelt B, Plum F. Whole-brain blood flow and oxygen metabolism in the rat during nitrous oxide anesthesia. *Am. J. Physiol.* 1975; 229: 113–8.
- Kershaw J, Nakamura K, Kondoh Y, Wakai A, Suzuki N, Kanno I. Confirming the existence of five peaks in ^{129}Xe rat head spectra. *Magn. Reson. Med.* 2007; 57: 791–7.

SUPPORTING INFORMATION

Additional supporting information may be found in the online version of this article at the publisher's web site.